Thermoplastic Composites Based on Poly(ethylene 2,6-naphthalate) and Basalt Woven Fabrics: Static and Dynamic Mechanical Properties

Luigi Sorrentino,[1,2] Davi Silva de Vasconcellos,[1] Marco D'Auria,[1,3] Fabrizio Sarasini,[4] Salvatore Iannace[1,2]

[1]*Istituto per i Polimeri, Compositi e Biomateriali, Consiglio Nazionale delle Ricerche, Piazzale E. Fermi 1, 80055 Portici (NA), Italy*

[2]*IMAST—Distretto Tecnologico sui Materiali e sulle Strutture, Napoli 80122, Italy*

[3]*Dipartimento di Ingegneria Chimica, dei Materiali e della Produzione Industriale, Università degli Studi di Napoli Federico II, Piazzale V. Tecchio 80, 80125 Napoli, Italy*

[4]*Dipartimento di Ingegneria Chimica, dei Materiali e dell'Ambiente, Università di Roma "La Sapienza", Via Eudossiana 18, 00184 Rome, Italy*

Composites based on poly(ethylene 2,6-naphthalate) and basalt woven fabrics have been investigated with the aim to develop composites with a minimum service temperature of 100°C. Laminates have been manufactured by using the film-stacking technique. A very low void content and a good fabric impregnation has been obtained as confirmed by the morphological analysis performed with scanning electron microscopy. Static flexural modulus and strength have been measured at 20, 60, and 100°C and compared with the dynamic mechanical behavior, evaluated from −100 to 220°C. A very good agreement has been detected between static and dynamic tests, proving that the dynamic mechanical analysis can be used to estimate the flexural modulus in a wide temperature range. Poly(ethylene 2,6-naphthalate)/basalt composites have exhibited (at 20°C) a flexural modulus and strength as high as 20 GPa and 320 MPa, respectively. The flexural modulus and the flexural strength at 100°C have been found to be equal to 18 GPa and 230 MPa, confirming that this system can retain very good mechanical properties at a service temperature of 100°C. POLYM. COMPOS., 00:000–000, 2015. © 2015 Society of Plastics Engineers

INTRODUCTION

Thermoplastic composites are still a niche market, occupying only 30% of the composites market [1] and are mainly used as secondary structural parts such as fixed wing leading edge, keel beams, and other small components, whereas exterior structural components in aeronautics are mostly based on thermoset matrices. As thermoset-based composites and their processes are a very mature technology, costs and weight reductions associated with design optimizations are ever more difficult to obtain, and as a consequence it is ever more difficult to meet incoming needs of an evolving aerospace environment with fixed structural costs. Reinforced thermoplastic composites offer the aerospace industry opportunities to couple structural performances to weight and cost savings and to a more environmental oriented technology with respect to thermosets [2]. In fact, raw thermoplastic matrices have a potential infinite shelf life, and thus cutting the low-temperature storage costs typical of thermoset resins or preimpregnated fibers. Thermoplastic polymers have increased impact resistance, higher damage tolerance, and interlaminar toughness owing to the presence of the amorphous phase that can retard the crack propagation and allow larger deformations [3]. They are potentially recyclable after their life cycle, have improved chemical and environmental resistance, and exhibit reduced moisture absorption [3]. Furthermore, they can be shaped and formed multiple times after being consolidated, and have the ability to be directly bonded without the use of adhesive layers, by means of fusion, induction, or resistance welding techniques. The increasing demand for high-performance composites from commodity market sectors can not only increase the overall composites market but also can boost the

Correspondence to: Luigi Sorrentino; e-mail: luigi.sorrentino@cnr.it
Contract grant sponsor: MIUR Ministry (Italy) within the TECOP project; contract grant number: PON02_00029_3206010.
DOI 10.1002/pc.23449
Published online in Wiley Online Library (wileyonlinelibrary.com).

adoption of thermoplastic composites as they allow a higher productivity with respect to thermosets. In fact, even if their production processes usually need expensive tools, they are suitable for high level of automation and hence high volume productions can be achieved.

Among the thermoplastic polymers, poly(ethylene 2,6-naphthalate) (PEN) is the most affordable high-performance polymer (when compared to polyphenylensulfide [PPS], polyetheretherketone [PEEK], polyetherimide [PEI], and polyethersulfone [PES]). As it has a glass transition temperature (T_g) >120°C, it is a good candidate for the production of high-performance/cost ratio composites with high service temperature. Its melting temperature is around 265°C and this in turn reduces the power requirements for its processing with respect to high-performance semicrystalline polymers such as PPS and PEEK. PEN has a very good thermal stability [4–6], it has very low moisture absorption [7] and, thanks to its semicrystalline structure, it can withstand a wide range of solvents. Currently, most applications of PEN are in the production of flexible electronic devices, such as flexible displays and photovoltaic cells, by large-scale manufacturing processes owing to the combination of properties such as ease of production process, good mechanical behavior, and reasonably high resistance to oxygen and water vapor penetration [8–10].

Only limited literature is available on the use of such polymer in composite applications. PEN has been used in continuous fiber form [11, 12] in composites based on epoxy resin, whereas it has recently been used as matrix for short fiber composites [13–15]. PEN has been used for the first time as matrix for continuous fiber composites by Sorrentino et al. [16], who prepared laminates based on glass fiber woven fabrics, and by Wang et al. [17] and Hine et al. [18], who focused on the preparation of a single polymer composite (albeit they were only able to use a single reinforcing layer).

Among all the reinforcing fibers, recently basalt fibers have gained an increasing attention as possible replacement for glass or carbon fibers [19–21] owing to their advantages in terms of environmental costs and chemico-physical properties. Mineral fibers obtained from basalt rocks are not new, but their suitability as reinforcement in polymer composites is a relatively new issue [22]. The chemical structure of basalt is similar to that of the glass although its density is slightly higher (>2.7 g/cm^3 compared to 2.54 g/cm^3 of glass) [23]. The chemical stability of basalt fibers is better than that of glass fibers, especially in an acidic environment [24]. They can also be used in a wide range of temperatures, from −200 to +600°C [20]. From the mechanical point of view, continuous basalt fibers are competitive with glass fibers. Their elastic modulus strongly depends on their chemical composition but it is usually equal or higher than that of glass fibers, whereas both tensile strength and elongation at break are higher [20, 25]. These characteristics make basalt fibers a promising reinforcing material in composites as confirmed by the growing attention that they are continuously gaining within the scientific community as reinforcement for both thermoplastic [21, 26–30] and thermosetting matrices [31–43].

The aim of this study has been to develop a thermoplastic composite capable of withstanding a service temperature of 100°C to permit its use in industrial applications where a high performance/cost ratio is needed and environmental aspects are limiting factors. To reach this goal, PEN as thermoplastic matrix and a basalt fiber woven fabric as reinforcement have been used to prepare composite laminates, which have been characterized under both static and dynamic loading conditions over a wide temperature range.

MATERIALS AND METHODS

Raw Materials

The thermoplastic matrix used for the laminate preparation has been the PEN homopolymer (Teonex TN8065S from Teijin Kasei, Japan). According to the manufacturer datasheet, this polymer has density of 1.35 g/cm^3 (25°C), T_g of 120°C, and T_m of 265°C. The basalt fiber reinforcement (BAS 220.1270.P) has been supplied by Basaltex-Flocart NV, Belgium. It is a plain weave fabric with surface weight of 220 g/m^2, yarn count of 7.2 ends/cm (warp and weft), and nominal thickness of 0.13 mm. According to the supplier data sheet, the basalt fibers employed (KVT150tex13-I) have density of 2.67 g/cm^3, average diameter of 13 ± 1.5 μm, Young's modulus of 85 ± 2 GPa, and melting point of 1,350 ± 100°C.

Materials Manufacturing

Thin films of neat PEN with a thickness of around 150 μm have been prepared by compression molding process. PEN pellets have been pressed at 300°C and 50 bar for 5 min, and then quenched. Unreinforced PEN plates have been produced as thermal reference for dynamic mechanical analysis (DMA) tests by using the same temperature and pressure profiles used for the laminates (see below). Composite plates were prepared by using the film-stacking process. All materials (PEN pellets and films, basalt fabrics) have been dried in an oven at 115°C with vacuum for at least 2 h. Eight layers of the reinforcing fabric have been alternatively stacked, with a 0/90° orientation of basalt woven fabric layers, between nine layers of PEN films in a mold with dimensions of 110 mm × 110 mm (length × width) and then pressed by using a hydraulic hot plate press (model P 300P, Collin GmbH, Germany). Temperature and pressure profiles have been optimized to obtain a very good impregnation of fibers. The processing sequence consists of a heating step at 300°C/1 bar for 5 min to melt the PEN films, followed by a compression step at 300°C/4 bar for 2 min to force

 DOI 10.1002/pc

the fabric's impregnation. At the end of the compression step, the mold with the composite plate has been quenched in cold water (at around 15°C), and thus forcing a fast cooling and hindering the formation of crystals in the polymer to obtain an almost amorphous matrix in the composite. The need for keeping PEN in the amorphous state is owing to the fact that the presence of crystals (ordered packing of a fraction of the thermoplastic macromolecules) increases the local density of the polymer and induces residual stresses that generate microcracks in the laminate during the used cooling process. To show the performance increase that can be potentially obtained from the maximization of the crystalline phase, semicrystalline specimens were obtained by annealing amorphous PEN specimens through an isothermal treatment operated at 180°C for 2 h.

Characterization Procedures

A morphological analysis with a scanning electron microscope has been performed on the samples to investigate the impregnation quality of the production process and the damaging of samples after the flexural characterization. Scanning electron microscopy (SEM) observations with a Quanta 200 FEG from FEI (Eindhoven, The Netherlands) were performed on gold-coated finely polished cross-sections.

Dynamic mechanical properties of both matrix and composites have been evaluated with a dynamic mechanical analyzer (TRITEC 2000 DMA, from Triton Technology, UK) by following the ASTM D 5023 Standard. DMA tests have been performed with a three-point bending configuration (dynamic displacement amplitude of 50 μm, frequency of 1 Hz) in a temperature range from −100 to 220°C (or until specimen failure) and using a heating rate of 2°C/min. Neat PEN specimens have been cut with dimensions of 32 mm × 10 mm × 1.0 mm and a support span of 20 mm has been used (span-to-depth ratio, 20:1). Composite specimens have been cut with dimensions of 43 mm × 12 mm × 1.6 mm with a support span of 25 mm (span-to-depth ratio, 16:1).

Static three-point bending tests have been performed according to the ASTM D790 Standard, by means of a universal testing machine (model 4304 from SANS—China, now MTS—USA) equipped with a 30 kN load cell and a climatic chamber. The loading nose and supports of the three-point bending fixture are made of stainless steel and have cylindrical surfaces with radius of curvature equal to 5 mm. Polymeric and composite samples (five samples for each temperature) with dimensions (length × width × thickness) of 127 mm × 12.7 mm × 3.2 mm and 100 mm × 12 mm × 1.6 mm, respectively, have been tested at 20°C. Composite samples were also tested at 60 and 100°C. The span-to-depth ratio used has been 32:1 for both polymeric and composite samples. The strain rate of the outer fibers during the laminates testing was equal to 0.01 mm/mm/min, which resulted in crosshead speed of 2.65 mm/min. Load–deflection curves have been plotted to determine the average values and standard deviation of the flexural strength (σ_y) and the flexural modulus of elasticity (E_B).

RESULTS AND DISCUSSION

Physical Properties of Materials and Reinforcement Impregnation

Composite plates presented an average thickness of 1.58 ± 0.05 mm and density of 1.82 ± 0.03 g/cm^3 (measured according to the ASTM D792 Standard). The average fiber weight ratio was $54.8 \pm 2.4\%$, corresponding to a fiber volume content of $37.5 \pm 2.2\%$, calculated using a matrix burn-off procedure (ASTM D3171 Standard). Composites' cross-sections were first qualitatively observed by an optical microscope to check for the presence of voids within fiber bundles and in the polymer matrix. The impregnation of fabrics resulted to be very good and no voids were detected by several optical acquisitions in any laminate and all bundles appeared to be well impregnated by the hosting matrix. The void volume content, calculated from the densities of components according to the ASTM D2734 Standard, was $1.5 \pm 0.7\%$.

The SEM analysis of laminates' cross-sections confirmed the very good fabric impregnation, which was uniform through the laminate thickness (Fig. 1a). The complete impregnation of yarns is confirmed by micrographs acquired at higher magnifications (Fig. 1b and c).

Dynamic Mechanical Analysis

DMA was performed from −100 to 220°C to evaluate the dependence of the laminate stiffness on the temperature. Unreinforced PEN was also tested to define the dynamic mechanical behavior of the matrix as reference for thermal transitions. In Fig. 2, the plots of the three-point bending DMA tests are presented for amorphous and semicrystalline polymer. The storage modulus, that can be considered as a rough estimation of the flexural modulus, of the amorphous PEN ranges from 4.5 to 1.5 GPa between −100°C and the occurrence of the curve onset (just above 100°C). The semicrystalline PEN showed a storage modulus increase of around 1.0 GPa through the same temperature range. Looking at tan δ, the amorphous PEN underwent a weak thermal transition around 50°C, whereas as the glass transition approached, a strong increase of tan δ occurred. The geometry used for the DMA testing prevented to detect the entire peak of tan δ curve of the amorphous PEN, being the sample stiffness well below the sensitivity of the testing analyzer. The semicrystalline PEN also showed the thermal transition around 50°C, but the curve onset, and hence the T_g increased of about 10°C with respect to the amorphous polymer. On the contrary, the storage modulus of the semicrystalline sample was still

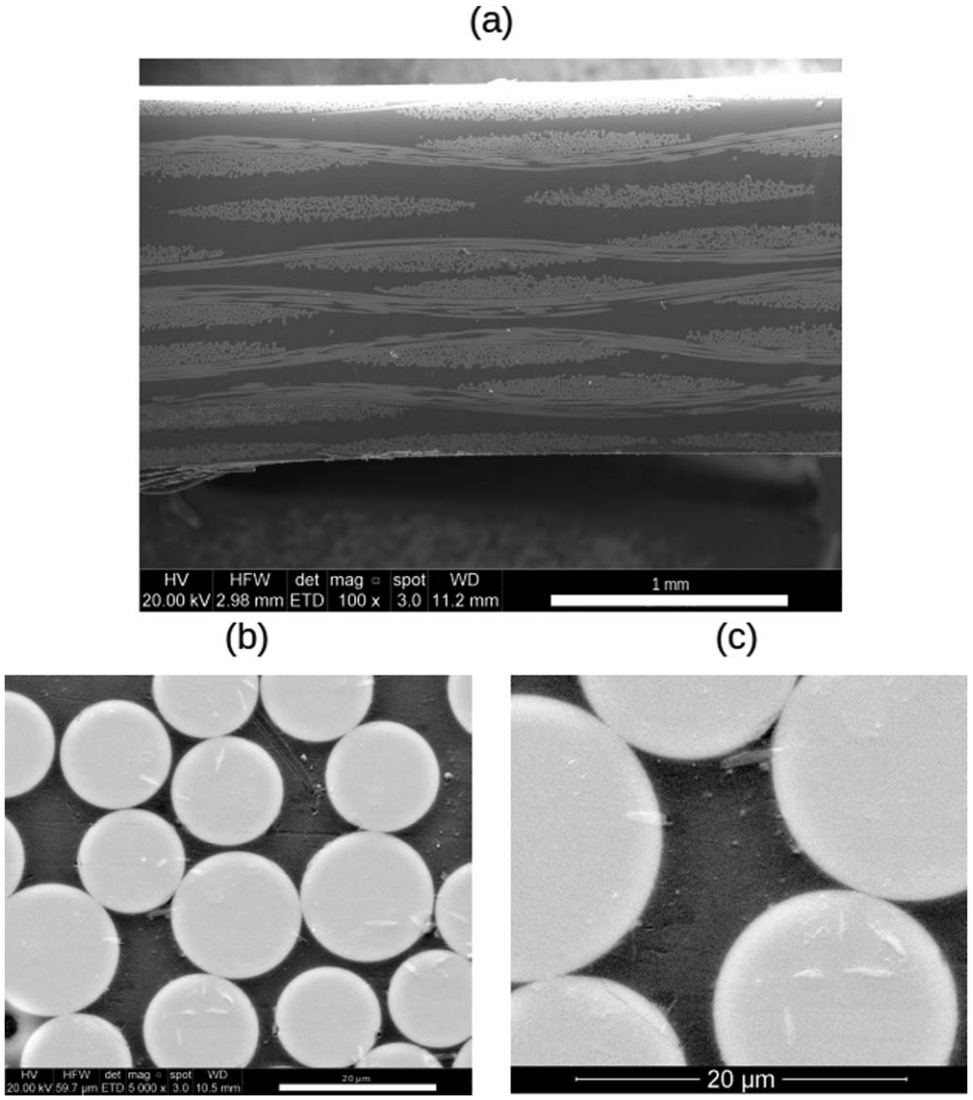

FIG. 1. SEM micrographs of laminate cross-sections at different magnifications: (a) 100 ×, (b) 5,000 ×, and (c) 10,000 ×.

measurable above the T_g, and decreased to 100 MPa at 220°C.

In Fig. 3, a typical curve from the three-point bending DMA test of basalt/amorphous PEN composite specimen is shown. The storage modulus of the laminate linearly decreased from around 26 to 20 GPa between −100°C and the occurrence of the curve onset. Above 100°C, a sharp drop was detected, referable to the DMA behavior of the amorphous PEN (Fig. 2). As the temperature reached 170°C, the crystallization of PEN occurred. The increase of the matrix stiffness (Fig. 2) affected the overall laminate response, which quickly rose up to 8.4 GPa at 180°C when the crystallization stopped, and then almost linearly decreased down to 7 GPa at 220°C. The tan δ curve of the composite showed a flat response until around 100°C and then a first peak at 120°C (T_g of PEN). A second peak of tan δ occurred at 150°C, referable to the formation and development of PEN crystals during the heating. These results show that both the amorphous

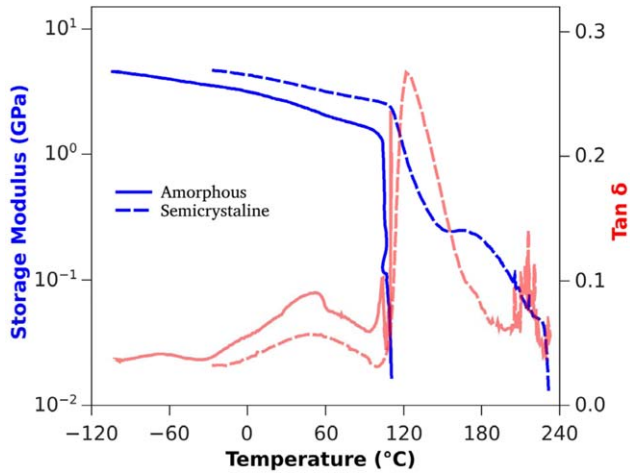

FIG. 2. DMA curves (storage modulus, loss modulus, and tan δ) of unreinforced amorphous and semicrystalline PEN. [Color figure can be viewed in the online issue, which is available at wileyonlinelibrary.com.]

DOI 10.1002/pc

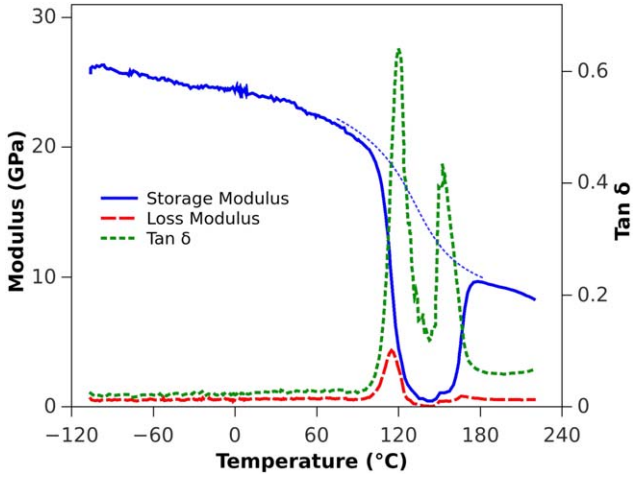

FIG. 3. DMA curves (storage modulus, loss modulus, and tan δ) of PEN/basalt composites. [Color figure can be viewed in the online issue, which is available at wileyonlinelibrary.com.]

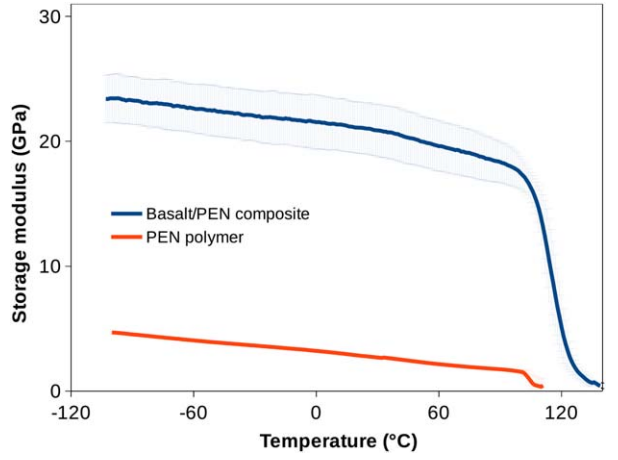

FIG. 4. Mean DMA curves and standard deviations of unreinforced amorphous PEN and PEN/basalt composite. [Color figure can be viewed in the online issue, which is available at wileyonlinelibrary.com.]

matrix and the amorphous composite retain a good stiffness (storage modulus) until around 100°C. After this temperature, the storage modulus decreases drastically, accompanied by a substantial increase of loss modulus and of tan δ as a consequence of the material entering in the rubbery region. The development of PEN crystals in the matrix, on the other hand, can result in a huge increase of the DMA response of the composite.

DMA tests are considered to correctly represent the influence of temperature on the elastic behavior of a material, but the absolute value of the elastic modulus measured by this technique usually differs from that measured by static mechanical tests although, in principle, they should be very similar. This discrepancy has been discussed by Deng et al. [44], who pointed out some reasons as machine compliance, test parameters, loading clamps, contact stresses, and specimen alignment. However, the use of the three-point bending configuration in the DMA can give results very close to those from static testing. Besides machine and test parameters, discrepancies in the absolute value of elastic modulus could also be related to specimen characteristics such as reinforcement orientation, dispersion on mechanical and physical properties, matrix impregnation, porosity, and geometry dimensions. To compensate these issues, in this study, DMA tests were performed on four specimens of each material (unreinforced PEN and basalt/PEN composite) and the mean curves of storage modulus versus temperature were calculated (Fig. 4). The standard deviation of the storage modulus for each temperature is also shown. A significant dispersion of storage modulus values is evident in the test results from the basalt/PEN composites with respect to those from the neat PEN polymer. The mean curve shape confirms the almost linear relationship of the storage modulus with the temperature range between −100 and 100°C, with a good retention of the stiffness for both materials. In Fig. 4, it is clear that the slopes of the linear part of the curves for neat PEN polymer and basalt/PEN composite are pretty similar, which allows to conclude that the dependence of the composite flexural behavior on the temperature is dominated by the thermoplastic matrix behavior. On the contrary, the stiffness data (absolute values of the storage modulus) are mostly dependent on the reinforcement properties.

Static Flexural Testing

The actual average values and standard deviations of the measured mechanical parameters (flexural modulus, flexural strength, and strain at yield) from static flexural tests of matrices (at 20°C) and composites (at 20, 60, and 100°C) are summarized in Table 1. It is worth noting that the flexural strength and the strain at yield have been considered as the stress and strain, respectively, at which the first visible load drop on the stress–strain curves has been detected as shown in Fig. 5. The semicrystalline PEN showed a higher flexural modulus with respect to the amorphous polymer, but both its strain at yield and its yield stress were significantly lower. Composite specimens tested at 20°C showed a mean flexural modulus of 20 GPa and a flexural strength of 320 MPa, both values comparable to those exhibited by epoxy resin/basalt composites [45]. The high flexural strength values confirm that the interface strength between PEN and the basalt

TABLE 1. Mean values and standard deviations of the flexural modulus (E_B), the flexural strength (σ_y), and the strain at yield (ε_y) at different temperatures.

Material	Temperature (°C)	E_B (GPa)	σ_y (MPa)	ε_y (%)
Matrix (amorphous)	20	2.20 ± 0.09	93.4 ± 0.8	4.94 ± 0.01
Matrix (semicrystalline)	20	3.40 ± 0.18	66.8 ± 5.7	1.89 ± 0.17
Basalt/PEN composite	20	20.3 ± 0.7	320 ± 12	1.82 ± 0.18
	60	19.4 ± 1.1	268 ± 17	1.54 ± 0.09
	100	18.1 ± 1.1	237 ± 29	1.85 ± 0.30

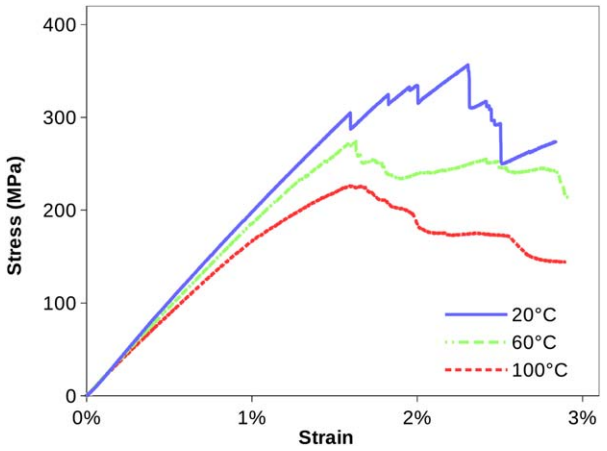

FIG. 5. Stress/strain curves from flexural tests on composites at 20, 60, and 100°C. [Color figure can be viewed in the online issue, which is available at wileyonlinelibrary.com.]

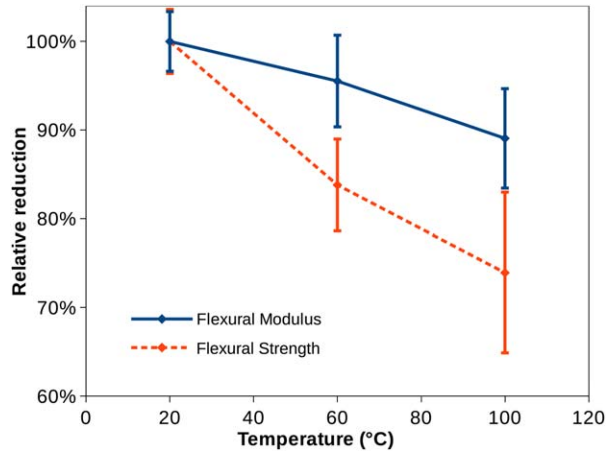

FIG. 6. Relative reduction of the flexural modulus and the flexural strength as function of the testing temperature. [Color figure can be viewed in the online issue, which is available at wileyonlinelibrary.com.]

fibers is very good in accordance with the findings from the morphological analysis. As the temperature rises, both the flexural modulus and the flexural strength reduce, down to 18.1 GPa and 237 MPa, respectively, at 100°C. In Fig. 6, the relative reductions of flexural modulus and strength are plotted as a function of the testing temperature and it shows that the flexural strength is more sensitive to the temperature than the flexural modulus as it undergoes a 17 and 26% reduction at 60 and 100°C, respectively, instead of 5 and 11% at the same temperatures for strength. The strain at yield does not show a clear dependence on the temperature ranging between 1.5 and 1.85%. The temperature affects the stress–strain curve

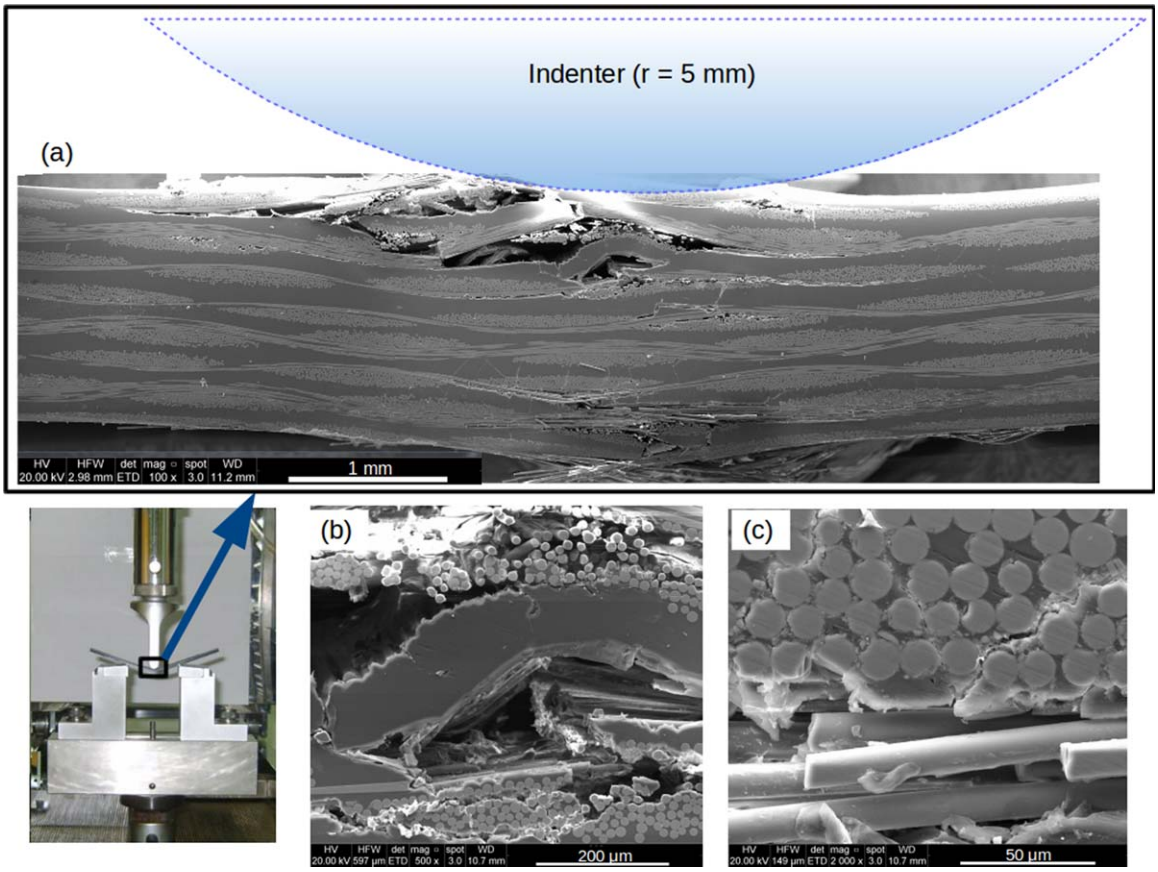

FIG. 7. SEM micrographs of a broken sample cross-section after the three-point bending test. [Color figure can be viewed in the online issue, which is available at wileyonlinelibrary.com.]

DOI 10.1002/pc

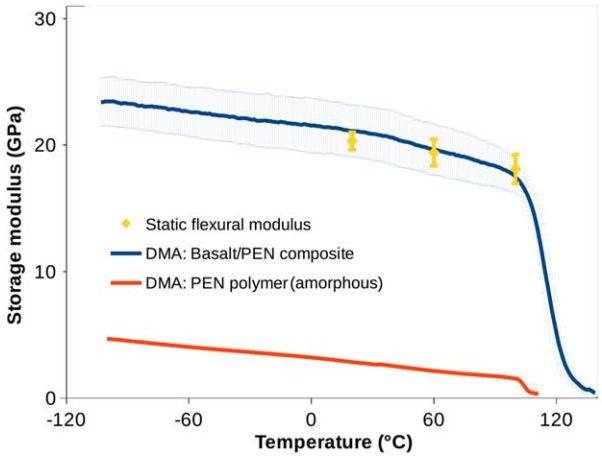

FIG. 8. Comparison of data from DMA and static flexural characterizations. [Color figure can be viewed in the online issue, which is available at wileyonlinelibrary.com.]

fluctuations as its rise leads to curves with reduced signal variability and more gradual stress decay (Fig. 5).

In the Fig. 7, SEM observations from a PEN/basalt composite after the bending test performed at room temperature are shown. Damage is characterized by local delaminations in the compression (upper) side, associated with fiber breakages owing to their buckling (Fig. 7b). In the tension (lower) side, there are fiber breakages in tension and orthogonal cracks in the matrix (Fig. 7c). Delaminations are localized in zones near the indenter tip (Fig. 7a), an indirect effect of the strong interface between PEN and fibers, which prevents damage from being spread along the sample length direction.

In Fig. 8, the measured values of the flexural modulus from the three-point bending analysis previously shown are plotted on DMA curves. This comparison shows a very good agreement between the static and the dynamic flexural moduli, with the DMA average curve that correctly fits the static values. In fact, despite of the larger variability of measured data, mean values are almost superimposed. This finding confirms that the DMA can be used as a reliable tool to evaluate the flexural modulus of the investigated thermoplastic composites. Based on this good correlation, data from crystallized PEN DMA tests can be used to estimate the flexural modulus at temperatures of $>100°C$ in composites with crystallized matrix (Fig. 3, dashed line). It is interesting to note that such material could theoretically exhibit flexural moduli as high as 8.4 ± 1.6 and 7.1 ± 1.5 GPa at 180 and 220°C, respectively, further extending the service temperatures of PEN/basalt composites.

CONCLUSIONS

Thermoplastic composites based on PEN and basalt woven fabrics with a fiber volume content higher than 37% have been successfully prepared by using the film-stacking technique. A very good impregnation with very low void content has been achieved as confirmed by SEM analysis and matrix burn-off tests. Composites have been characterized under static and dynamic mechanical conditions. DMA tests have shown that the developed composites show high storage moduli up to 100°C, and, although a drop occurs across the T_g of the PEN, a storage modulus as high as 8.4 GPa can be achieved after the formation of the crystalline phase in PEN. The static flexural modulus, evaluated at 20, 60, and 100°C, has shown a very good agreement with the DMA data, and thus confirming that DMA can be used to estimate the flexural modulus of PEN/basalt composites as a function of the temperature. The flexural modulus and the flexural strength at 20°C (20.3 GPa and 320 MPa, respectively) are comparable with those exhibited by similarly reinforced thermoset composites based on epoxy resin and basalt woven fabrics. The flexural performance of the developed laminates at 100°C has been equal to 18 GPa and 230 MPa for modulus and strength, respectively, and thus confirming that this system can retain good mechanical properties at a service temperature of at least 100°C.

ACKNOWLEDGMENT

The authors thank Fabio Docimo for his contribution to the preparation of all tested samples.

REFERENCES

1. M. Biron, *Thermoplastics and Thermoplastic Composites*, Elsevier, Amsterdam (2012).
2. F. Touchard, M.C. Lafarie-Frenot, and D. Guédra-Degeorges, *Compos. Sci. Technol.*, **56**, 785 (1996).
3. G. Simeoli, D. Acierno, C. Meola, L. Sorrentino, S. Iannace, and P. Russo, *Compos. Part B Eng.*, **62**, 88 (2014).
4. G. Botelho, A. Queirós, and P. Gijsman, *Polym. Degrad. Stab.*, **70**, 299 (2000).
5. L. Turnbull, J.J. Liggat, and W.A. MacDonald, *Polym. Degrad. Stab.*, **98**, 2244 (2013).
6. A. Arkhireyeva and S. Hashemi, *Polymer*, **43**, 289 (2002).
7. Y. Aoki, L. Li, T. Amari, K. Nishimura, and Y. Arashiro, *Macromolecules*, **32**, 1923 (1999).
8. A. Tonelli, *Polymer*, **43**, 637 (2002).
9. S.R. Forrest, *Nature*, **428**, 911 (2004).
10. Y. Galagan, J.-E.J.M. Rubingh, R. Andriessen, C.-C. Fan, P.W.M. Blom, S.C. Veenstra, and J.M. Kroon, *Sol. Energy Mater. Sol. Cells*, **95**, 1339 (2011).
11. C. Lechat, A.R. Bunsell, P. Davies, and A. Piant, *J. Mater. Sci.*, **41**, 1745 (2006).
12. M. Afshari, P. Chen, and R. Kotek, *J. Appl. Polym. Sci.*, **125**, 2271 (2012).
13. L. Zheng, J. Qi, D. Liu, and W. Zhou, *J. Appl. Polym. Sci.*, **112**, 3462 (2009).
14. N.G. Karsli, S. Yesil, and A. Aytac, *Mater. Des.*, **46**, 867 (2013).
15. C. Xu, L. Cao, and Y. Chen, *Polym. Compos.*, **35**, 5 (2014).

16. L. Sorrentino, L. Cafiero, M. D'Auria, and S. Iannace, *Compos. Part A: Appl. Sci. Manuf.*, **64**, 223 (2014).
17. J. Wang, J. Chen, and P. Dai, *Compos. Sci. Technol.*, **91**, 50 (2014).
18. P.J. Hine, A. Astruc, and I.M. Ward, *J. Appl. Polym. Sci.*, **93**, 796 (2004).
19. T. Czigany, *eXPRESS Polym. Lett.*, **1**, 59 (2007).
20. T. Deak and T. Czigany, *Text. Res. J.*, **79**, 645 (2009).
21. T. Czigány, J. Vad, and K. Pölöskei, *Mech. Eng.*, **49**, 3 (2005).
22. A. Ross, *Compos. Technol.*, **12**, 4 (2006).
23. L. Van de Velde, V.K. Kiekens, P. Van Langenhove, *Proceedings of the 10th International Conference on Composite Engineering*, University of New Orleans, New Orleans, 5 (2003).
24. B. Wei, H. Cao, and S. Song, *Mater. Sci. Eng. A*, **527**, 4708 (2010).
25. A. Dorigato and A. Pegoretti, *J. Compos. Mater.*, **46**, 1773 (2012).
26. J. Szabó and T. Czigány, *Polym. Test.*, **22**, 711 (2003).
27. F. Ronkay and T. Czigány, *Polym. Adv. Technol.*, **17**, 830 (2006).
28. T. Czigány, *Compos. Sci. Technol.*, **66**, 3210 (2006).
29. T. Liu, F. Yu, X. Yu, and X. Zhao, *J. Appl. Polym. Sci.*, **125**, 1292 (2012).
30. Y. Zhang, C. Yu, P.K. Chu, F. Lv, C. Zhang, J. Ji, R. Zhang, and H. Wang, *Mater. Chem. Phys.*, **133**, 845 (2012).
31. T. Czigány, K. Pölöskei, and J. Karger-Kocsis, *J. Mater. Sci.* **40**, 5609 (2005).
32. M. Wang, Z. Zhang, Y. Li, M. Li, and Z. Sun, *J. Reinf. Plast. Compos.*, **27**, 393 (2008).
33. Q. Liu and M. Shaw, *Polym. Compos.*, **27**, 1 (2006).
34. Q. Liu and M. Shaw, *Polym. Compos.*, **27**, 475 (2006).
35. S. Carmisciano, I.M. De Rosa, F. Sarasini, A. Tamburrano, and M. Valente, *Mater. Des.* **32**, 337 (2011).
36. V. Lopresto, C. Leone, and I. De Iorio, *Compos. Part B Eng.*, **42**, 717 (2011).
37. C. Colombo, L. Vergani, and M. Burman, *Compos. Struct.*, **94**, 1165 (2012).
38. J.H. Lee, K.Y. Rhee, and S.J. Park, *Mater. Sci. Eng. A*, **527**, 6838 (2010).
39. H. Li, G. Xian, Q. Lin, and H. Zhang, *J. Appl. Polym. Sci.*, **123**, 3781 (2012).
40. L. Yusriah, M. Mariatti, and A. Abu Bakar, *J. Reinf. Plast. Compos.*, **29**, 3066 (2010).
41. S. Sfarra, C. Ibarra-Castanedo, C. Santulli, A. Paoletti, D. Paoletti, F. Sarasini, A. Bendada, and X. Maldague, *Compos. Part B Eng.*, **45**, 601 (2013).
42. I.A. Subagia, L. Tijing, and Y. Kim, *Compos. Part B Eng.*, **58**, 611 (2014).
43. F. Sarasini, J. Tirillò, L. Ferrante, M. Valente, T. Valente, L. Lampani, P. Gaudenzi, S. Cioffi, S. Iannace, and L. Sorrentino, *Compos. Part B Eng.*, **59**, 204 (2014).
44. S. Deng, M. Hou, and L. Ye, *Polym. Test.*, **26**, 803 (2007).
45. F. Sarasini, J. Tirillò, M. Valente, and T. Valente, *Compos. Part A: Appl. Sci. Manuf.*, **47**, 109 (2013).

 DOI 10.1002/pc